PERGAMON

International Journal of Multiphase Flow 28 (2002) 1381–1407

International Journal of Multiphase Flow

www.elsevier.com/locate/ijmulflow

Modelling hydrodynamics and turbulence in a bubble column using the Euler–Lagrange procedure

S. Laín [a,b], D. Bröder [a], M. Sommerfeld [a,*], M.F. Göz [a]

[a] *Lehrstuhl MVT, Institut für Verfahrenstechnik, Fachbereich Ingenieurwissenschaften Martin-Luther-Universität Halle-Wittenberg, D-06099 Halle (Saale), Germany*

[b] *Laboratory of Research on Combustion Tecnologies, LITEC-CSIC, C/María de Luna 10, 50015 Zaragoza, Spain*

Received 23 August 2001; received in revised form 4 April 2002

Abstract

This paper describes an extension and validation of the Euler/Lagrange approach for time-dependent calculations of the flow evolving in a bubble column. The continuous phase velocity is obtained by solving the two-dimensional axisymmetric Reynolds-averaged Navier–Stokes equations augmented by the k–ε turbulence model. The coupling between the phases is considered through momentum source terms and source terms in the k- and ε-equations, which include the effect of wake-generated turbulence by means of consistent Lagrangian-like terms. Bubble motion is calculated by solving the equations of motion taking into account drag force, liquid inertia, added mass, buoyancy and gravity, and the transverse lift force. In order to identify the relative importance of the different physical phenomena involved in the model, the radial variation of the corresponding constitutive terms that appear in the transport equations of the liquid variables is analyzed in an instantaneous as well as in the time-averaged configuration. As a conclusion, the bubble source terms are directly responsible for the production of fluctuating kinetic energy and dissipation rate in the liquid, which means that their modelling determines the topology of the liquid flow in the bubble column. For validation the numerical results are quantitatively compared with detailed measurements utilizing phase-Doppler anemometry.

Keywords: Bubble column; Hydrodynamics; Numerical calculation; Euler–Lagrange approach; Turbulence modelling

* Corresponding author. Tel.: +49-3461-462-879; fax: +49-3461-462-878.
E-mail address: martin.sommerfeld@iw.uni-halle.de (M. Sommerfeld).

0301-9322/02/$ - see front matter
PII: S0301-9322(02)00028-9

1. Introduction

Bubbly flows occur in a variety of industrial processes, such as elaboration of alloys, two-phase heat exchangers, aeration and stirring of reactors, flotation devices, and bubble column reactors. Bubble columns, in which a large number of gas bubbles rise through a liquid, are frequently encountered in the chemical, petrochemical and biotechnological industries. They are used in many chemical processes, for instance Fischer–Tropsch synthesis, manufacture of fine chemicals, oxidation reactions, coal liquefaction, and fermentation reactions. The main advantages of bubble column reactors are, from the apparatus side, the relatively simple construction and the absence of mechanically moving parts meaning easy maintenance and low operating costs, and with regard to the internal flow and efficiency behaviour, large interfacial area and transport rates leading to excellent heat and mass transfer characteristics.

For the sound design and use of bubble columns in process engineering it is necessary to understand their fundamental hydrodynamic behaviour, which is determined by bubble rise, bubble–bubble and bubble–fluid interactions, bubble size and size distribution, and gas hold-up. However, the investigation of the interaction and resulting collective motion of bubbles, together with its influence on the evolution of large-scale flow structures, in dependence upon bubble size and deformability as well as voidage is only at its beginning (Bunner and Tryggvason, 1999; Göz et al., 2000; Bunner, 2000). Moreover, turbulence is induced in the liquid by the movement of the bubbles due to shear produced in the vicinity of the bubbles, in particular due to bubble oscillations and wakes. Although several attempts to account for bubble- or particle-induced turbulence have been presented in the literature (Yuan and Michaelides, 1992; Kenning and Crowe, 1997; Crowe and Gillandt, 1998; Février and Simonin, 1998), a reliable and generally accepted model is still lacking.

While the time-averaged flow within a bubble column shows a very regular and symmetric structure, the transient flow behaviour is generally highly irregular and asymmetric (cf. e.g. Tzeng et al., 1993; Devanathan et al., 1995). As the dispersed elements react to local and instantaneous flow patterns (brought about mainly by themselves in this case) and not to averaged ones, the dynamic interactions among bubbles and between bubbles and liquid affect the performance of the column; since this is a continual process, where a steady state is reached in the statistical sense at best, it will in general be inadequate to perform stationary calculations. Instead time-dependent simulations are required to obtain detailed information on the hydrodynamic behaviour, from which then time-averaged quantities like mean bubble rise velocity, mean liquid kinetic energy, and transport parameters, as well as corresponding fluctuation quantities can be derived. Concerning asymmetry, fully three-dimensional calculations are desirable but may be inhibited by computational restrictions; for cylindrical columns two-dimensional axisymmetric simulations seem to give satisfactory results (Sanyal et al., 1999) and therefore, to be suited enough.

Bubbly flows can be simulated in various ways, with different levels of approximation and complexity. Most fundamental are direct numerical simulations which resolve all scales of the flow around and inside finite-sized and deformable bubbles (Delnoij et al., 1997a; Esmaeeli and Tryggvason, 1999). This approach provides the most detailed insight into single-bubble dynamics as well as into bubble–bubble and bubble–fluid interactions. It may be used to evaluate the influence of basic physical and geometric parameters like inertia, viscosity, surface tension, bubble size and gas volume fraction on the evolution of bubble swarms, the interaction of bubbles of different

sizes, and the induced flow structure of the liquid (Bunner and Tryggvason, 1999; Göz et al., 2000; Bunner, 2000). Since this direct approach is restricted to the simulation of relatively few bubbles (Bunner and Tryggvason, 1998), the flow in an entire bubble column must be calculated by other means involving necessarily some kind of coarsening or averaging. As such, Euler/Lagrange and Euler/Euler methods are available, both with or without turbulence modelling to avoid the numerical resolution of very small flow scales.

The next coarser level after direct numerical simulations is represented by the models of Euler/Lagrange type (Delnoij et al., 1997b; Sommerfeld, 1996). In this approach, the fluid flow is described by the Navier–Stokes equations, while the dispersed elements (solid particles, drops, or bubbles) moving through the fluid are tracked explicitly by solving their Newtonian equations of motion. These equations have to contain all relevant forces applied by the surrounding liquid on a gas bubble and external field forces. Conversely, in order to ensure two-way coupling between the phases, a momentum source term has to be introduced into the Navier–Stokes equation accounting for the momentum transfer from the bubbles to the liquid. Usually the bubbles are treated as point-like, in the sense that their size and shape enter the interaction terms only implicitly via the semi-empirical drag coefficient. Direct bubble–bubble interactions may be taken into account via a collision model; in this case the Euler/Lagrange method is currently restricted to the simulation of dilute flows due to the high computational load.

Euler/Euler or two-fluid models are derived either by volume- or ensemble-averaging the basic Euler–Lagrange equations (Jackson, 1997; Aliod and Dopazo, 1990; Prosperetti and Zhang, 1994), or by employing a kinetic transport equation for a probability density function for the dispersed elements (Zaichik and Alipchenkov, 1999; Reeks, 1993; Hyland et al., 1998). These methods lead to a set of Navier–Stokes-like equations for the two phases, which are coupled by phase interaction terms. These interaction terms look naturally similar to the force terms appearing in the Lagrangian description of a single bubble moving in a continuous liquid, but have to be modified to take account of the local voidage distribution (i.e. of the effect of neighbouring bubbles on a given one). In addition, a similar closure problem arises as in single-phase turbulence modelling, because the averaging procedure gives rise to pseudo-turbulent Reynolds stresses involving averages of products of velocity fluctuations. Euler/Euler models are well suited for the description and computation of dense flows (e.g. fluidized beds); they have also been used successfully for dilute flows, although their validity becomes questionable in the very dilute limit. The clear advantage of such models is their computational efficiency and that they are amenable to analytic investigations (see e.g. Göz and Sundaresan, 1998 and the references therein), which allow to study the emergence and stability of global flow patterns. On the other hand, it is easy to account for a wide spectrum of bubble sizes and incorporate models for bubble/drop breakup and coalescence using the Euler/Lagrange approach, whereas the Euler/Euler approach requires that each size class be represented by an extra set of equations.

The derivation of turbulence models is a formidable task in both of these simplifying approaches. For an Euler/Euler model time-averaged equations of coupled two-fluid equations have to be derived and closed. This has been attempted for instance by Simonin (Février and Simonin, 1998; Simonin, 1990) and Crowe and Gillandt (1998), and in the more general framework of kinetic theory by Reeks (Reeks, 1993; Hyland et al., 1998) and Zaichik and Alipchenkov (1999). The results of these studies are more or less similar but cannot be considered completely satisfactory so far, which is to be blamed on the extremely complicated nature of the problem. In an

Euler/Lagrange approach there is only one continuous fluid, so adopting a single-phase turbulence model for this fluid suggests itself. However, the source terms and effective transport coefficients belonging to such a turbulence model have to be modified appropriately to account for the presence and action of the bubbles. In addition, the fluid velocity appearing in the bubble momentum equation will be composed of a local mean value obtained from the Reynolds-averaged Navier–Stokes equations and a fluctuating component generated e.g. by a Langevin model (Sommerfeld, 1993; Shirolkar et al., 1996). These modelling issues are far from being solved; for instance, there are strong indications that apparent constants appearing in a k–ε turbulence model actually depend on voidage and bubble size (Squires and Eaton, 1992; Kohnen, 1997).

While it is obvious that all these model proposals have to be checked against experiments, detailed quantitative comparisons of computational results with experimental data are scarce in the case of bubble columns. Dynamic simulations of gas–liquid flows in bubble columns have certainly received appreciable attention during the recent years. Most simulations, however, were restricted to two-dimensional or axisymmetric calculations, and comparisons with experiments stayed mostly on the qualitative level. On the other hand, detailed measurements of liquid and bubble velocities and turbulence intensities for columns of different sizes and under different operating conditions were carried out only recently, thus providing a data base for further investigations (Lin et al., 1996; Mudde et al., 1997, Bröder and Sommerfeld, 1998).

Lübbert and coworkers performed time-dependent simulations of two- (Lapin and Lübbert, 1994) and three-dimensional (Devanathan et al., 1995) bubble columns based on a simplified Euler–Lagrange representation, where the bubbles were described by spatial density distributions reacting to buoyancy. Their calculations of bubble paths, transient velocity and density patterns revealed the chaotic nature of the flow. Sokolichin and Eigenberger (1994) used an Euler–Euler model for the laminar simulation of a uniformly aerated two-dimensional bubble column. The results for a locally aerated column were compared with corresponding experiments in a flat bubble column (Becker et al., 1994). While good qualitative agreement of the long-time averaged as well as the transient flow behaviour was found, the value of the liquid viscosity had to be increased by a factor of 100 to obtain satisfying quantitative agreement in the liquid velocity field. Delnoij et al. discussed a hierarchy of models corresponding to the three levels of approach described above (Delnoij et al., 1997a–c). Single-bubble dynamics and two-bubble interactions were simulated directly using a volume-of-fluid method for interface tracking. With their Euler–Lagrange or discrete bubble model they studied the effect of column aspect ratio on the global flow structure and also compared the results, mostly in a qualitative way, of two-dimensional simulations with the experiments of Becker et al. (1994) in a locally aerated flat column.

A number of very recent studies have employed turbulence models and also provided detailed comparisons of simulation results with experimental data. Sokolichin and Eigenberger (1999) included the standard k–ε model in a simplified Euler/Euler approach, in which constant slip velocity between the two phases is assumed. They brought forth the insufficiency of two-dimensional simulations but found good agreement of time- and depth-averaged liquid velocity profiles obtained from three-dimensional simulations with the measurements of Becker et al. (1994). Pan et al. (1999) used a two-fluid model supplied with a model for bubble-induced turbulent viscosity of the liquid phase to analyze the characteristics of large-scale flow structures in two-dimensional bubble columns. Their findings on wavelength and frequency of the meandering central plume,

mean velocities, and turbulence intensities are in fair agreement with the experiments of Lin et al. (1996) and Mudde et al. (1997). Sanyal et al. (1999) used an algebraic slip mixture model as well as a two-fluid model with a set of modified k–ε equations to include interphase turbulent momentum transfer. They performed two-dimensional axisymmetric simulations in the bubbly flow and churn-turbulent regimes and obtained reasonable quantitative agreement of time-averaged gas hold-up, axial liquid velocity, and turbulent kinetic energy profiles with own experimental data obtained by means of CARPT techniques. Data collected under a variety of operating conditions, distributors and column sizes, and across various flow regimes show that, in a time-averaged sense, the liquid goes up at the center of the column and descends at the walls in a single-recirculation loop. Such circulation shows a symmetric axial–radial dependence alone, being the instantaneous azimuthal component of velocity not significant in determining the time-averaged flow profile. In addition, azimuthal–radial components of time-average liquid velocity are significantly smaller than axial components. Therefore, these authors conclude that, despite the fact that the flow in bubble columns is highly turbulent and chaotic, being the transient flow asymmetric about the central axis, the time-averaged flow is roughly symmetric.

Following this line of thinking, the Euler/Lagrange approach with k–ε turbulence model was extended by Laín et al. (1999) to account for turbulence modification by the bubbles. Interphase coupling was considered through momentum source terms and source terms in the k- and ε-equations. Two-dimensional, instationary, axisymmetric calculations of the flow evolving in a cylindrical bubble column were performed for different closure assumptions and compared with experimental values. The results revealed a strong dependence of the mean and fluctuating bubble velocity components on the drag law and the modelling of the source term in the equation for the turbulent kinetic energy. Moreover, it was shown that a bubble size distribution needs to be considered for reproducing the non-isotropic nature of bubble velocity fluctuations seen in the experiments.

The present paper provides a more detailed study of the modelling of bubble-induced turbulence within the Euler/Lagrange framework. Also, performing a two-dimensional transient axisymmetric calculation, this work compares against detailed experimental data not only the bubble variables but also the liquid fields, showing a reasonable agreement in all considered quantities. Special emphasis is made on the modelling of the interaction terms in the liquid turbulent energy. A source term for the kinetic energy of the continuous phase similar to the one proposed by Crowe and Gillandt (1998) (given in an Euler/Euler approach) but able to incorporate the effect of all the forces considered in the bubble momentum equation, is derived and validated quantitatively against detailed experimental measurements. This contribution is expressed in terms of Lagrangian quantities, so their implementation in the Euler/Lagrange procedure is straightforward. Moreover, in order to get more insight into the underlying mechanisms governing the exchange of momentum and turbulent kinetic energy between the liquid and bubble phases, the transport equations for the liquid phase are split into their five global contributions (explicit time derivative, convection, diffusion, source and interaction terms) and their relative importance is analysed.

After briefly mentioning the experimental background, the basic model and the numerical approach will be described in Section 3. Models to account for the effect of the bubbles on the liquid turbulence will be discussed in Section 4. Section 5 contains the evaluation of the numerical results and Section 6 the conclusions.

2. Experimental background

A scheme of the experimental setup is shown in Fig. 1. The cylindrical bubble column has a diameter of 140 mm and a height of 650 mm (water level in the column). Aeration is performed by means of a porous membrane with a diameter of 100 mm and pore sizes of 0.7 μm. The gas flow rate is varied through the supply pressure.

A two-component fibre optics PDA was used to measure bubble sizes and velocities as well as liquid velocities at four cross-sections above the aerator, namely at 30, 100, 300 and 480 mm. In order to reduce refraction effects of the laser beams at the curved wall of the bubble column, it was placed in a square vessel also filled with tap water. The selected optical configuration of the PDA-system allowed for a sizing range of up to 2 mm (Bröder and Sommerfeld, 1998). The measurement of the liquid-phase velocities was achieved by adding fluorescing tracer particles to the liquid.

The results of various experiments with different gas hold-up and bubble size distributions were published previously and will therefore be used here only for comparison with numerical simulations. A detailed description of the measurement technique and numerous results can be found in Bröder et al. (2000); measured bubble rise velocities and bubble fluctuating velocity components in comparison with simulation results were presented in Laín et al. (1999).

3. Basic model and numerical approach

The dynamic simulation of the flow evolving in a bubble column has been performed using the Euler/Lagrange approach. The fluid flow was calculated by solving the unsteady Reynolds-averaged conservation equations. These equations were closed using the well-known k–ε turbu-

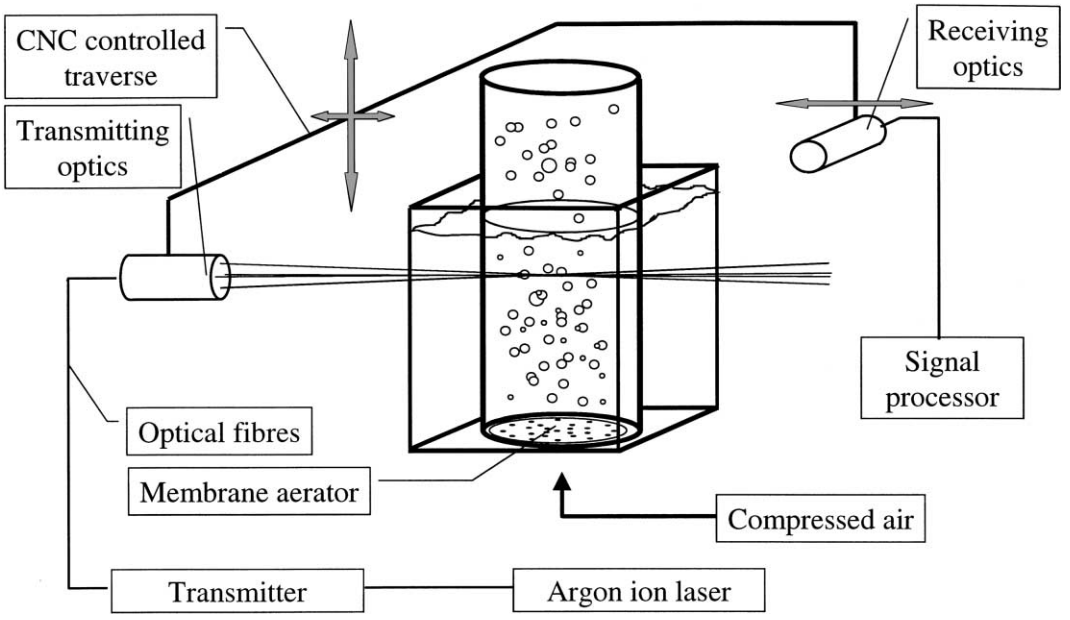

Fig. 1. The bubble column experimental facility with PDA setup.

lence model (Launder and Spalding, 1974), extended by accounting for the effects of the dispersed phase. The time-dependent conservation equations for the fluid in a two-dimensional axisymmetric flow may be written in the general form:

$$(\varrho\phi)_{,t} + (\varrho U_i\phi)_{,i} = (\Gamma\phi_{,i})_{,i} + S_\phi + S_{\phi\mathrm{B}} \tag{1}$$

Here, ϱ is the liquid density, U_i ($i = x, r, \varphi$) are the Reynolds-averaged velocity components (also denoted U, V, W), and Γ is an effective transport coefficient. The usual source terms within the continuous phase are collected in S_ϕ, while $S_{\phi\mathrm{B}}$ represents the additional source term due to phase interaction. In Eq. (1) the usual tensorial notation is assumed, where the comma followed by a subscript means partial derivative and summation is performed over repeated indexes. Table 1 summarizes the meaning of these quantities for the different variables ϕ in the case of axisymmetric flow.

Since at present only low void fractions are considered, lower than 2% in all the considered cases, the liquid density is assumed to be unaffected by the presence of the bubbles. The resulting set of equations is solved by using a finite volume discretisation scheme and applying an iterative solution procedure based on the SIMPLE algorithm. The time derivatives are discretised using the fully implicit method, while the diffusive and the convective terms are discretised using central and hybrid differences, respectively.

The simulation of the bubble phase by the Lagrangian method requires the solution of the equation of motion for each computational bubble (representing a parcel of real bubbles with

Table 1
Summary of terms in the general equation for the different variables that describe the liquid phase in axisymmetric flow

ϕ	Γ	S_ϕ	$S_{\phi\mathrm{B}}$
1	–	0	$S_{\varrho\mathrm{B}} = 0$
U	$\mu + \mu_t$	$\frac{\partial}{\partial x}\left(\Gamma\frac{\partial U}{\partial x}\right) + \frac{1}{r}\frac{\partial}{\partial r}\left(r\Gamma\frac{\partial V}{\partial x}\right) - \frac{\partial p}{\partial x} + \rho g_x$	$S_{U\mathrm{B}}$
V	$\mu + \mu_t$	$\frac{\partial}{\partial x}\left(\Gamma\frac{\partial U}{\partial r}\right) + \frac{1}{r}\frac{\partial}{\partial r}\left(r\Gamma\frac{\partial V}{\partial r}\right) - \frac{\partial p}{\partial r} - 2\Gamma\frac{V}{r^2} + \rho\frac{W^2}{r}$	$S_{V\mathrm{B}}$
W	$\mu + \mu_t$	$-\rho\frac{VW}{r} - \frac{W}{r^2}\frac{\partial}{\partial r}(\Gamma r)$	$S_{W\mathrm{B}}$
k	$\mu + \frac{\mu_t}{\sigma_k}$	$G_k - \varrho\varepsilon$	$S_{k\mathrm{B}}$
ε	$\mu + \frac{\mu_t}{\sigma_\varepsilon}$	$\frac{\varepsilon}{k}(C_1 G_k - C_2\varrho\varepsilon)$	$S_{\varepsilon\mathrm{B}}$

$$G_k = \mu_t\left\{2\left[\left(\frac{\partial U}{\partial x}\right)^2 + \left(\frac{\partial V}{\partial r}\right)^2 + \left(\frac{V}{r}\right)^2\right] + \left(\frac{\partial U}{\partial r} + \frac{\partial V}{\partial x}\right)^2 + \left(\frac{\partial W}{\partial x}\right)^2 + \left(r\frac{\partial}{\partial r}\left(\frac{W}{r}\right)\right)^2\right\}$$

$$\mu_t = C_{\mu\varrho}\frac{k^2}{\varepsilon}$$

$$C_\mu = 0.09;\ C_1 = 1.44;\ C_2 = 1.92;\ \sigma_k = 1.0;\ \sigma_\varepsilon = 1.3$$

identical properties). Depending on bubble size and void fraction typically between 10 000 and 20 000 computational bubbles were simultaneously present in the flow field. The bubble motion after injection is calculated by solving the following set of ordinary differential equations:

$$\frac{\mathrm{d}x_{\mathrm{B}i}}{\mathrm{d}t} = u_{\mathrm{B}i} \tag{2}$$

$$\underbrace{m_{\mathrm{B}}\frac{\mathrm{d}u_{\mathrm{B}i}}{\mathrm{d}t}}_{\mathscr{A}} = \underbrace{\frac{3}{4}\frac{\varrho}{\varrho_{\mathrm{B}}D_{\mathrm{B}}}m_{\mathrm{B}}C_{\mathrm{D}}(u_i-u_{\mathrm{B}i})|\mathbf{u}-\mathbf{u}_{\mathrm{B}}|}_{\mathscr{B}} + \underbrace{m_{\mathrm{B}}g_i\left(1-\frac{\varrho}{\varrho_{\mathrm{B}}}\right)}_{\mathscr{C}} + \underbrace{\frac{1}{2}m_{\mathrm{B}}\frac{\varrho}{\varrho_{\mathrm{B}}}\left(\frac{\mathscr{D}u_i}{\mathscr{D}t}-\frac{\mathrm{d}u_{\mathrm{B}i}}{\mathrm{d}t}\right)}_{\mathscr{D}}$$
$$+ \underbrace{\frac{1}{2}m_{\mathrm{B}}\frac{\varrho}{\varrho_{\mathrm{B}}}\epsilon_{ijk}\epsilon_{klm}(u_j-u_{\mathrm{B}j})\frac{\partial u_l}{\partial x_m}}_{\mathscr{E}} + \underbrace{m_{\mathrm{B}}\frac{\varrho}{\varrho_{\mathrm{B}}}\frac{\mathscr{D}u_i}{\mathscr{D}t}}_{\mathscr{F}} \tag{3}$$

with $\mathscr{A}$, inertia force acting on the bubble due to its acceleration, $\mathscr{B}$, force due to drag, $\mathscr{C}$, force due to gravity and buoyancy, $\mathscr{D}$, force due to virtual mass effect, $\mathscr{E}$, force due to transverse lift, and $\mathscr{F}$, force due to pressure gradient.

Other forces such as the Basset history term are assumed to be negligible. Here, $x_{\mathrm{B}i}$ are the coordinates of the bubble position, $u_{\mathrm{B}i}$ are the velocity components, D_{B} is the bubble diameter, and ϱ_{B} is the gas density which is assumed to be constant at present. The symbol $\mathscr{D}\cdot/\mathscr{D}t$ means the derivative following the fluid element. ϵ_{ijk} are the components of the Levi–Civita pseudo-tensor (equal to 1 when ijk is an even permutation of 123, -1 when the permutation is odd, and zero when any two indexes have the same value), which are used to express the curl or the cross-product of vectors. As in the previous work (Laín et al., 1999) the drag coefficient C_{D} is calculated using the empirical correlations for a fluid sphere:

$$C_{\mathrm{D}} = \begin{cases} 16Re_{\mathrm{B}}^{-1} & Re_{\mathrm{B}} < 1.5 \\ 14.9Re_{\mathrm{B}}^{-0.78} & 1.5 < Re_{\mathrm{B}} < 80 \\ 48Re_{\mathrm{B}}^{-1}(1-2.21Re_{\mathrm{B}}^{-0.5}) + 1.86\times10^{-15}Re_{\mathrm{B}}^{4.756} & 80 < Re_{\mathrm{B}} < 1500 \\ 2.61 & 1500 < Re_{\mathrm{B}} \end{cases} \tag{4}$$

where $Re_{\mathrm{B}} = \varrho D_{\mathrm{B}}|\mathbf{u}-\mathbf{u}_{\mathrm{B}}|/\mu$ is the bubble Reynolds number.

The instantaneous fluid velocity at the bubble location occurring in Eq. (3) is determined from the local mean fluid velocity linearly interpolated from the neighbouring grid points and a fluctuating component generated by the Langevin model described by Sommerfeld (1993). In this model the fluctuating velocity is composed of a part that is correlated to the value at the previous time step and a random component sampled from a Gaussian distribution function. The correlated part is calculated using appropriate turbulent time and length scales obtained from the k–ε turbulence model.

The equation of motion is analytically integrated by assuming that the forces such as gravity and buoyancy, virtual mass, transverse lift and pressure term are constant during the time step. The resulting equation is discretised and solved using a first-order Euler method. The numerical solution requires that the time step of integration (i.e. the Lagrangian time step Δt_{L}) is sufficiently smaller than all relevant time scales for the bubble motion, namely:

- the time required for a bubble to cross a control volume,
- the bubble response time scale,

$$\tau_B(C_D) = \frac{4}{3\mu} \frac{(\varrho_B + 0.5\varrho)D_B^2}{Re_B C_D} \tag{5}$$

- the integral time scale of turbulence which varies along the trajectory due to the consideration of local values for k and ε is given by:

$$T_e = 0.16\frac{k}{\varepsilon}$$

where k and ε are evaluated in the location of the bubble being linearly interpolated from the neighbouring grid points.

In order to avoid numerical instabilities, the time step was limited to be 25% of the minimum of the above given time scales (Laín and Göz, 2001). For improving numerical efficiency the Lagrangian time step was not fixed, but allowed to vary along the bubble trajectory.

4. Effect of the bubbles on the liquid velocity fluctuations

Since the liquid flow in the bubble column is driven by the bubble rise, the source terms due to the bubble phase are essential. As both phases are computed time-dependent and sequential (Fig. 2a,b), the evaluation of the source terms and the coupling between the phases requires some special treatment in order to yield reasonable averages of the source terms for each control volume, in which bubbles are present.

The selected Eulerian time step (Δt_E) determines the temporal resolution of the flow fluctuations and was selected in the range between 0.05 and 0.5 s, however most of the computations were performed with a time step of 0.05 s. Since the Lagrangian time step (Δt_L) for calculating the bubble trajectories is generally much smaller (i.e. in the range of 10^{-4} s, typical ratio

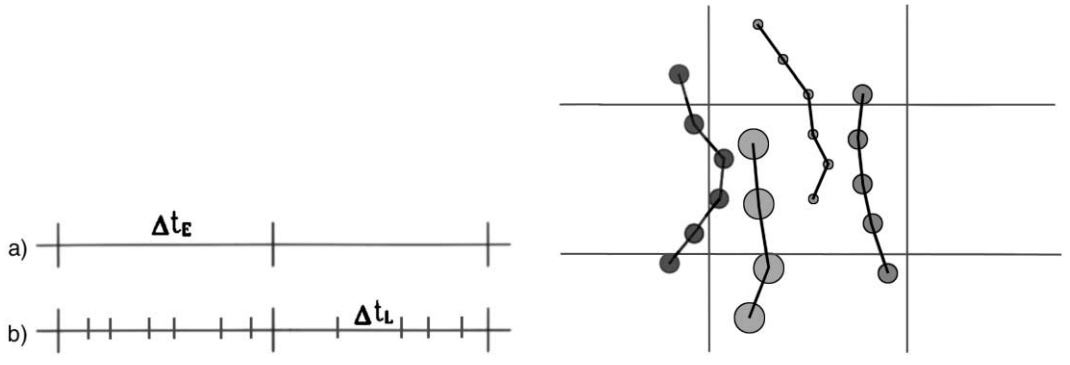

Fig. 2. Left: (a) Eulerian time step used in the time-dependent solution of transport equations (1); (b) Lagrangian time steps used in the bubble tracking. Right: Illustration of the averaging of the source terms along the bubble trajectory during an Eulerian time step.

$\Delta t_E/\Delta t_L \gg 50$–$100$) this selection yields appropriate temporal averaging of the source terms as it will be described below.

The calculation of the interaction terms is realised by means of the particle-source-in-cell (PSI-cell) approximation of Crowe et al. (1977). This model considers the dispersed phase as a local source of momentum, turbulent energy and dissipation of kinetic turbulent energy. In this context, the expression for the momentum equation source term due to the bubbles is obtained by time- and ensemble-averaging in the following form (Gouesbet and Berlemont, 1999):

$$\overline{S_{U_i\mathrm{B}}} = -\frac{1}{V_{\mathrm{cv}}\Delta t_{\mathrm{E}}}\sum_k m_k N_k \sum_n \left\{ \left([u_{\mathrm{B}i}]_k^{n+1} - [u_{\mathrm{B}i}]_k^n \right) - g_i \left(1 - \frac{\varrho}{\varrho_{\mathrm{B}}} \right) \Delta t_{\mathrm{L}} \right\} \tag{6}$$

where the sum over n indicates averaging of the instantaneous momentum contributions $S_{U_i\mathrm{B}}$ along the bubble trajectory (i.e. time-averaging) and the sum over k is related to the number of computational bubbles passing through the considered control volume of size V_{cv} (Fig. 2, right). The mass of an individual bubble is given by m_k, while N_k is the number of real bubbles contained in one computational bubble. In (6) only the contact forces have to be taken into account, so the external forces have to be subtracted.

Following the PSI-cell strategy, the coupling terms are introduced only within the cell where the centre of gravity is located. Let us remark that in Eq. (6) the temporal change of the instantaneous bubble velocity is taken instead of the forces acting on such bubble, because from a Lagrangian perspective it is easier and automatically all forces are accounted for.

The modification of the liquid turbulence by the bubbles is accounted for by appropriate source terms in the k- and ε-equations. Initially, two approaches have been considered:

1. The source term resulting from the Reynolds-averaging procedure (6), which is related to the momentum transfer between the phases, is given by (Gouesbet and Berlemont, 1999)

$$S_{k\mathrm{B}} = \overline{u_i S_{U_i\mathrm{B}}} - U_i \overline{S_{U_i\mathrm{B}}} \tag{7}$$

   where summation is implicit in the index i. In the Lagrangian frame the correlations are evaluated by using the instantaneous values. In the following this expression will be referred to as the *standard terms* because they are of frequent use in the literature. One particularity of these terms is that they can only predict suppression of continuous phase turbulence due to their structure. Moreover, Crowe (2000) has shown that this terms provide incorrect values under theoretical limiting conditions.
2. The source term proposed by Crowe and Gillandt (1998) derived originally for gas–solid flows, which can be interpreted as an energy balance, is expressed in terms of volume averages as

$$S_{k\mathrm{B}} = \frac{\alpha_{\mathrm{B}}\varrho_{\mathrm{B}}}{\tau_{\mathrm{B}}(C_{\mathrm{D}})}\left\{ |\langle u_i\rangle - \langle u_{\mathrm{B}i}\rangle|^2 + (\langle u'_{\mathrm{B}i}u'_{\mathrm{B}i}\rangle - \langle u'_i u'_{\mathrm{B}i}\rangle) \right\} \tag{8}$$

   The first contribution, proportional to the square of the relative mean velocity between the bubbles and the liquid, reflects the conversion of mechanical work done by the drag force into turbulent kinetic energy and is thus supposed to take account of wake-induced turbulence. The second term represents a redistribution of the kinetic turbulent energy between the phases. In this formula α_{B} is a mean volume fraction of gas and $\tau_{\mathrm{B}}(C_{\mathrm{D}})$ is a mean bubble response time

scale; the dependency of the latter on drag coefficient and Reynolds number can be identified from Eqs. (4) and (5). Expression (8) will be named *Crowe terms* hereafter.

The modelling of the analogous term in the ε-equation is performed in the standard manner, which assumes that the additional production or destruction of dissipation is proportional to $S_{k\mathrm{B}}$ and the inverse of the Lagrangian turbulent characteristic time scale $C_{\mathrm{L}}k/\varepsilon$ (Gouesbet and Berlemont, 1999). Grouping the coefficient C_{L} with the proportionality constant, it is possible to write

$$S_{\varepsilon\mathrm{B}} = C_{\varepsilon 3}\frac{\varepsilon}{k}S_{k\mathrm{B}} \tag{9}$$

The adequacy of expression (9) is controversial, in particular in combination with the *standard term* (7). Squires and Eaton (1992) note that (9) is an ad hoc parametrization of the effect of particles (or bubbles) on the dissipation rate and conclude from comparisons with direct numerical simulations that the value for the constant $C_{\varepsilon 3}$ is not universal, but depends most likely on volume fraction and particle diameter. Moreover, following these authors, negative values of $C_{\varepsilon 3}$ are necessary to represent the effect of particles in flows where they act as a source of ε, because as it has been said previously, the model (7) assumes that the particles provide a sink for the dissipation rate and thus yields negative values of $S_{k\mathrm{B}}$. However, this does not necessarily invalidate the ansatz (9); rather the applicability of (7) is apparently restricted. The Crowe term, on the other hand, considers the particles mostly as a source of dissipation, as only the last part of (8) may give a negative contribution to $S_{k\mathrm{B}}$. Therefore, and in absence of more comprehensive theoretical results, Eq. (9) has been used in the present approach though not without caution. A study of the dependence of the flow field topology on the value of $C_{\varepsilon 3}$ has been carried out and will be presented below. Most of the calculations have been performed with a value of 1.8, which will be justified below.

The use of the Crowe terms (8), originally developed for gas–solids flow, in conjunction with the bubble equation of motion (3) is not fully consistent, because in the derivation of (8) the added mass and transverse lift forces have not been considered. Therefore, these forces are involved in the calculation of the bubble trajectories but not in the two-way coupling, i.e. their effect does not appear in the interaction source term $S_{k\mathrm{B}}$. One way to recover consistency would be to repeat the Eulerian-like procedure described in Crowe and Gillandt (1998) taking also into account the other contact forces besides drag. Unfortunately, this is not an easy task mainly due to the unsteady nature of the added mass force and the final expression can be quite complicated. A noteworthy first though not complete approach can be found in Zaichik and Alipchenkov (1999).

In order to include all considered forces in the two-way coupling from a Lagrangian perspective, it is necessary to look closer to the structure of the interaction terms obtained by Reynolds-averaging. Following Ishii (1975, 1990), for any given reference point ($\mathbf{x}$, t), there are definite times $t_1,\ t_2, \ldots, t_n$ in the interval between $(t - \Delta t/2)$ and $(t + \Delta t/2)$ (Δt is the interval of averaging) at which interfaces pass the point $\mathbf{x}$. The interaction term is then defined as an average over discrete boundary values at point $\mathbf{x}$ (occurring at times $t_1, t_2, \ldots, t_n$) of the corresponding variable ϕ during the continuous (Eulerian) time interval Δt.

From this point of view, the average appearing in the first term of (7), $\overline{u_i S_{U_i\mathrm{B}}}$, is taken over the set of events in which there is an interface present at the point $\mathbf{x}$ during Δt. However, as long as mass transfer is not considered, the instantaneous velocities of both phases must coincide at the

interface, i.e. $u_i|_s = u_{Bi}|_s$. If rotation and deformation of the discrete elements are neglected, this velocity must coincide with the velocity of the center of mass of the bubble u_{Bi}. Therefore, substituting the instantaneous liquid velocity by the bubble velocity in (7) the following expression is obtained:

$$S_{k\mathrm{B}} = \overline{u_{Bi} S_{U_i\mathrm{B}}} - U_i \overline{S_{U_i\mathrm{B}}} \tag{10}$$

which is easily evaluated in a Lagrangian framework. It is necessary to remark that $S_{U_i\mathrm{B}}$ represents the instantaneous contact force that the discrete element exerts on the fluid. Then, it is not difficult to realise that if only the drag force is considered in $S_{U_i\mathrm{B}}$ with the Crowe and Gillandt assumptions of monodispersed spherical particles, Eq. (10) reduces to the *Crowe terms* (8). In addition, (10) includes, in a natural way and Lagrangian language, the contribution of the other forces introduced in the bubble motion equation to the modulation of the turbulent kinetic energy k. In the following, Eq. (10) will be referred to as the *consistent terms*.

It should be noted, however, that (10) constitutes only a first approximation to $S_{k\mathrm{B}}$ as long as rotation and deformation of the dispersed elements are not yet considered. Nevertheless, in the cases treated here, the bubbles can be assumed to be spherical and their rotation can be neglected, so the use of (10) is sufficiently justified.

5. Boundary and initial conditions: computational procedure

The bubble column of diameter 140 mm and height 650 mm was discretised by employing uniform grid with 150×25 cells in the axial and radial direction respectively. For demonstrating the grid independence of the results also a grid of 220×35 cells was considered for one case. The boundary conditions employed for the continuous phase are:

- symmetry conditions with zero gradient of the liquid-phase properties and zero radial velocity on the centre line,
- wall boundary conditions at the bottom and side wall,
- the free surface of the bubble column was also specified as a wall boundary condition, which implies a no-slip condition.

The bubbles were injected just above the bottom of the bubble column over a cross-section with a diameter of 100 mm according to the experiments. The gas-phase mass flux was constant across the aerator. Two experimental cases were considered with a gas flow rate of 15 l/h (case 1) and 87 l/h (case 2) which results in gas-phase volume fractions of about 0.37% and 1.31%, respectively. The size of the bubble was sampled stochastically from the measured size distribution which was very similar in both cases (i.e. a rather narrow distribution in the range between 0.2 and 0.9 mm with a number mean diameter of 0.5 mm). In the calculations the size distribution was discretised by seven size classes of 0.1 mm width. The initial bubble velocity was sampled from a Gaussian distribution with a mean and rms value corresponding to the measurements. At the free surface of course the bubbles are leaving the computational domain.

The calculation procedure is briefly summarised in the following. Firstly, the bubbles are randomly injected at the inlet area and tracked in quiescent liquid for a duration corresponding to

the Eulerian time step in order to evaluate the source terms described above. During this first step of the start-up period of course the bubbles do not yet reach the surface of the column. These source terms are used to calculate the fluid flow field until a converged solution is achieved. Then the Lagrangian tracking with injecting new bubbles in each time step is continued. With the new source terms the flow field at the next time level is calculated and so forth (Fig. 2a,b). It should be mentioned that with this unsteady procedure no under-relaxation of the source terms should be used.

The evolution of the quasi-steady flow in the bubble column begins when the first bubbles leave the column. Normally this situation is reached after about 10 s. At this stage typically 20 000 computational bubbles are included in the entire flow field. The determination of the time-averaged liquid- and bubble-phase properties begins when the flow pattern is established and a single-recirculation loop exists in the bubble column typically after about 400 s. The averaging time for the properties of both phases is about 200 s.

The typical temporal evolution of the flow structure in the bubble column is shown in Fig. 3 by plotting the velocity vectors. One half of the bubble column is shown here, with the wall being located at the left side and the symmetry axis at the right. It should be noted that these figures are quasi-instantaneous velocity fields obtained during an Eulerian time step after the specified time levels. The over-all flow pattern shows one large recirculation loop with some fluctuations in the up- and down-flow regions. The temporal evolution of the cumulative axial mean velocity profile for case 1 at a location 480 mm above the aeration for three time steps is shown in Fig. 4. This result reveals some stronger changes between 100 and 200 s. However, the variation of the cumulative liquid velocity after 200 s is only very small. Similarly the cumulative bubble mean velocity in the upward direction at a given monitoring location shows stronger fluctuations only during the first 200 s (Fig. 5). Thereafter, some smaller velocity variations are observed and a quasi-steady bubble velocity is achieved after 700 s.

The effect of grid size is assessed by plotting the profile of the averaged axial liquid velocity 480 mm above the aerator after a time period of 200 s (Fig. 6). The difference between both profiles is very small, revealing that the coarser grid (i.e. 150×25 nodes) provides an appropriate discretisation of the calculation domain. Similarly the liquid velocity fluctuations showed only very small differences for the two grids considered (not shown here). Therefore, the results presented in the following were obtained with a resolution of 150×25 grid nodes in the axial and radial direction, respectively.

The dependency of the axial mean liquid velocity on the length of Eulerian time step at the location of 480 mm above the aerator is illustrated in Fig. 7. A large time step implies a poorer resolution of the unsteady behaviour of the bubble column dynamics, while a shorter time step will allow to resolve the small time scale structures. As it can be seen from the plot, an Eulerian time step of 0.05 s is enough to assure a proper resolution of temporal structures and it will be taken in the rest of the simulations.

6. Results

In a previous work (Laín et al., 1999) the feasibility of the Euler/Lagrange approach, in connection with a turbulence model including the *Crowe terms* (8), to describe the main phenomena

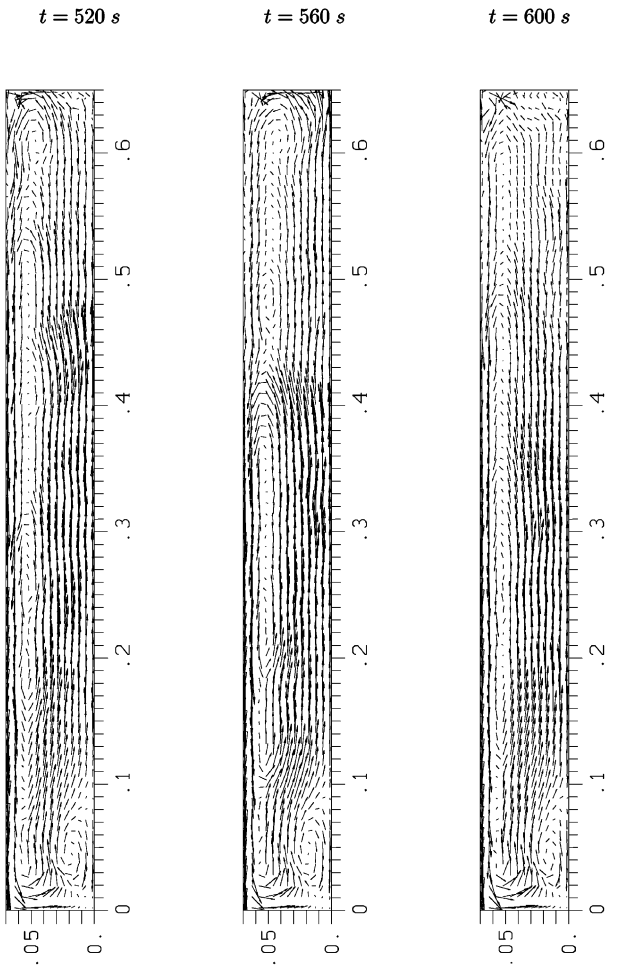

Fig. 3. Instantaneous plots of the liquid velocity field at three equidistant times for the case of gas volume fraction 0.37%.

occuring in a bubble column was assessed by comparing calculated mean and fluctuating bubble velocities with experimental measurements. A parametric study as well as a study of the effect of different modelling alternatives was also performed. The main conclusions obtained were the following:

1. A polydispersed size distribution of bubbles had to be used in order to obtain the experimentally observed anisotropy in the bubble fluctuating velocity components.
2. The drag correlations for fluid spheres were necessary to predict the bubble's rising velocity correctly in comparison to own measurements.
3. The use of the *standard terms* showed a considerable underprediction of the fluctuating bubble velocity, whereas the *Crowe terms* provided a better approximation.

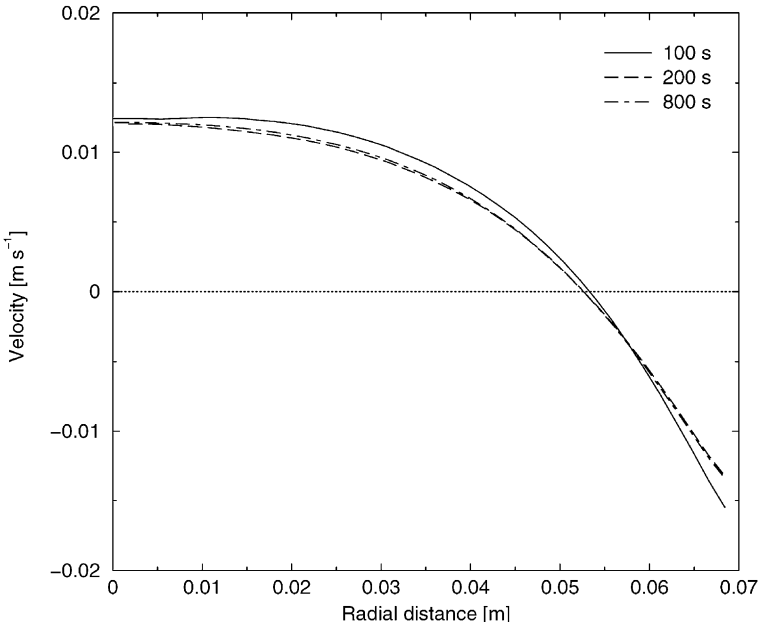

Fig. 4. Influence of the total real time of the simulation on the mean velocities (case 15 l/h). Axial liquid mean velocity profile at 480 mm above the aerator for the three different total times considered.

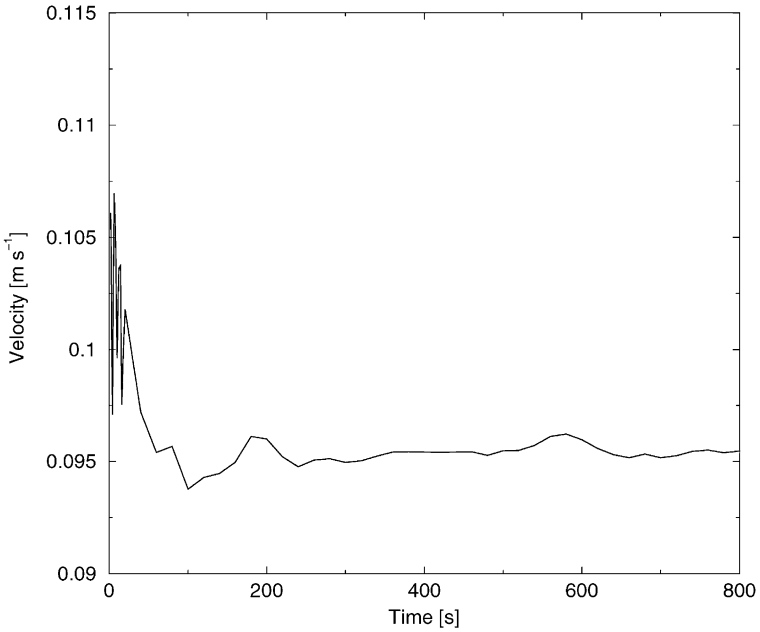

Fig. 5. Influence of the total real time of the simulation on the mean velocities (case 15 l/h). Cumulative average of the axial bubble mean velocity at the monitoring point $x = 480$ mm, $r = 4$ mm.

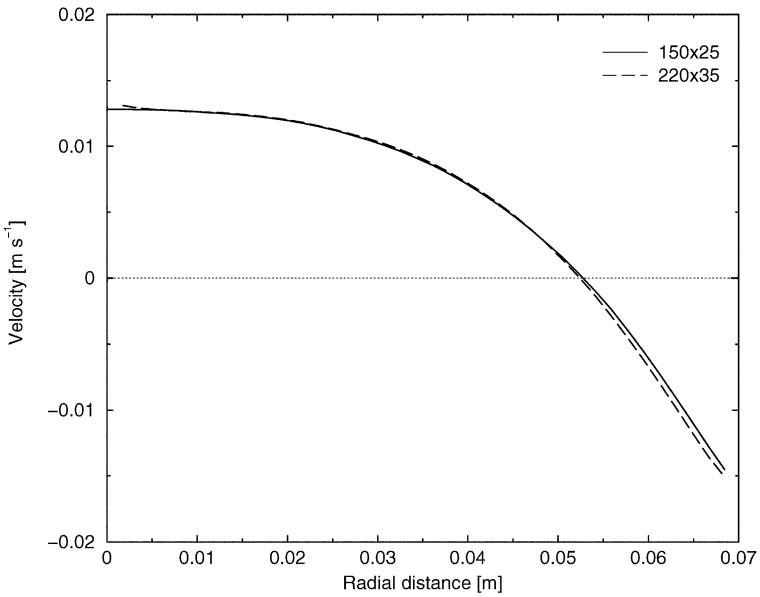

Fig. 6. Axial liquid mean velocity at 480 mm above the aerator for the two different grids considered (case 15 l/h, 200 s of total averaging time).

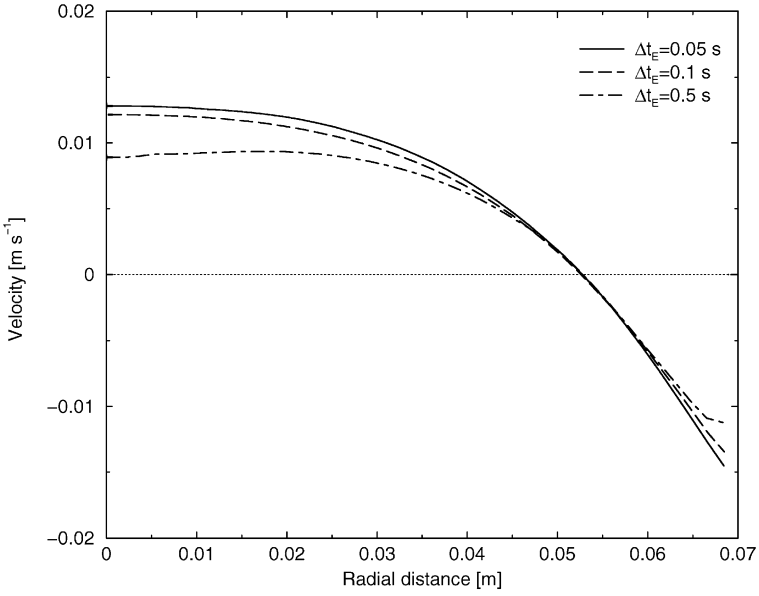

Fig. 7. Influence on the axial liquid mean velocity (section 480 mm above the aerator) on the Eulerian time step employed for the solution of the transport equations (1) (case 15 l/h, 200 s of total averaging time).

The inadequacy of the *standard terms* in the configuration of bubble column reactor is not surprising because the motion of the fluid is exclusively due to the bubbles motion. In addition,

Crowe (2000) has shown that these terms, which always subtract fluctuating energy of the continuous phase, lead to a fallacy under limiting conditions, so they are not correct.

In the present work, comparisons not only with bubble velocities but also with mean and fluctuating liquid velocities are carried out using the *consistent terms* (10) to describe the effects of the bubbles on the turbulent structure of the liquid phase.

6.1. Comparison of simulations and experiment

Quantitative comparisons of the radial variation of time-averaged quantities between the experiments and the simulations results will be presented mainly for the upper bubble column cross-section, i.e. 480 mm above the aerator. Fig. 8 summarizes the results for both void fractions. In the case of the lower void fraction (left) a good agreement in the bubble axial mean and fluctuating velocities is found. Also the mean velocity of the liquid is predicted satisfactorily, capturing in particular the point in which the upward fluid flow changes to downwards near the wall. The turbulent energy of the liquid velocity is also reasonably well captured.

A comparison of the influence of the source terms in the turbulent kinetic energy equation is shown in Fig. 9 for case 1 (i.e. volume fraction 0.37%). It is obvious, that the *standard terms*, Eq. (7), yield to a complete underprediction of the velocity fluctuation of the liquid phase and a complete destruction of the flow structure. Namely the mean liquid velocity profile reveals a down-flow in the core of the bubble column. Moreover, the bubble-phase mean and fluctuation velocities in the streamwise direction are remarkably underpredicted.

The right part of Fig. 8 presents the performance of the simulations against the experiments for the 1.31% gas volume fraction case. Here, the mean velocity of the bubbles is overpredicted and that of the liquid is underpredicted, while the fluctuating components differ only slightly from the measured values. The deviations are probably due to a slight underprediction of dissipation

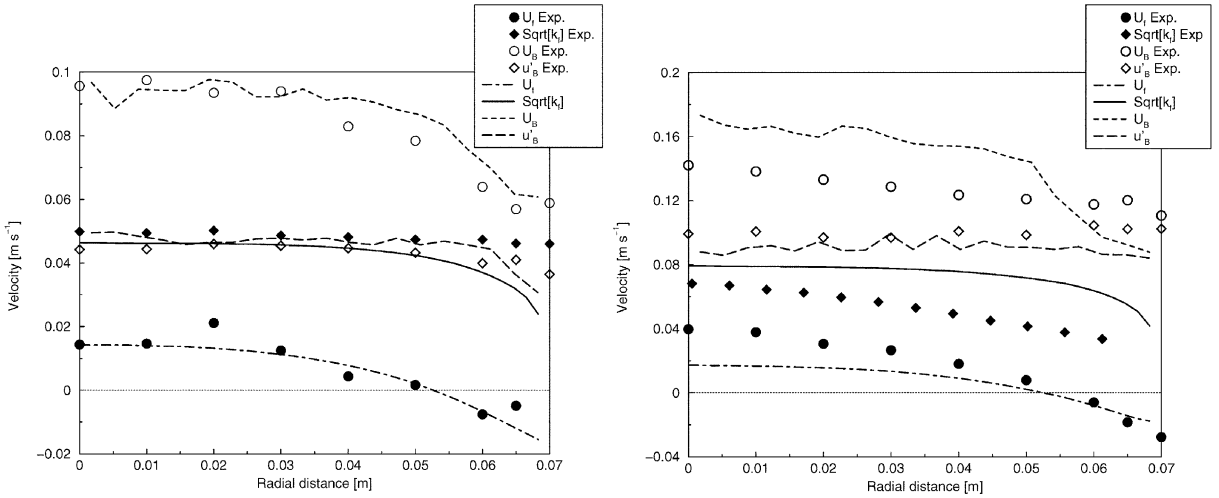

Fig. 8. Mean and fluctuating axial velocities of gas and liquid phase for gas volume fractions of 0.37% (left) and 1.31% (right) at $x = 480$ mm above the aerator. Calculations have been carried out with the *consistent terms*.

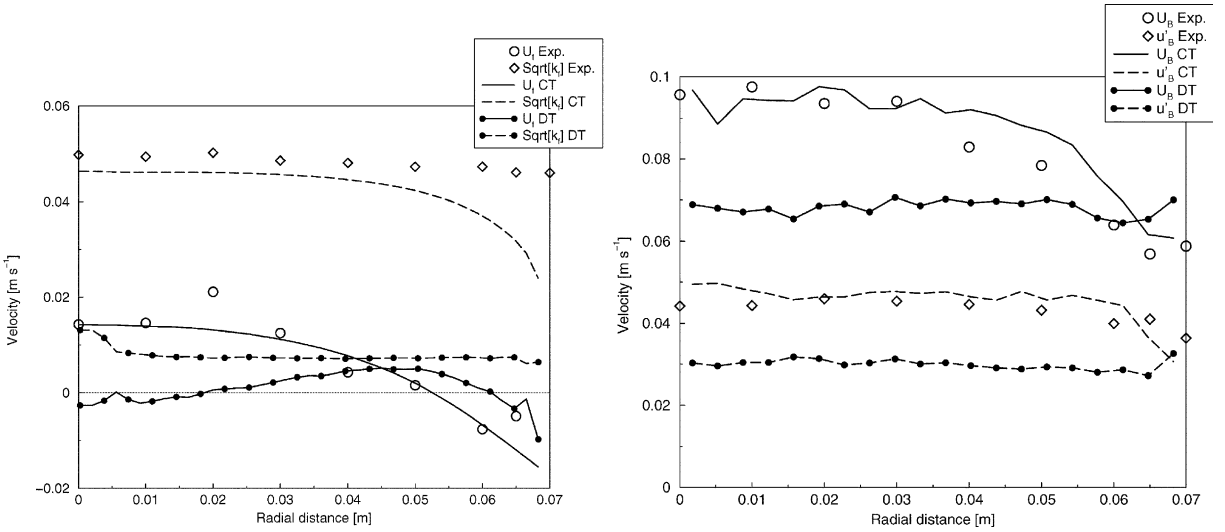

Fig. 9. Performance of the consistent bubble source terms in the k- and ε-equations ('CT' in the plot) versus the standard Reynolds-averaged terms ('DT') for the case of 0.37% gas void fraction. Left: fluid variables, right: bubble velocities.

induced by the bubbles on the liquid. It is to be mentioned that in these two simulations a value of $C_{\varepsilon 3} = 1.8$ has been used, but as it has been said before, this value likely depends on the voidage.

In addition, the evolution of profiles along the axis of the bubble column is presented in Fig. 10 for the case of 15 l/h. The meaning of the symbols is the same as in Fig. 8. Reasonable agreement

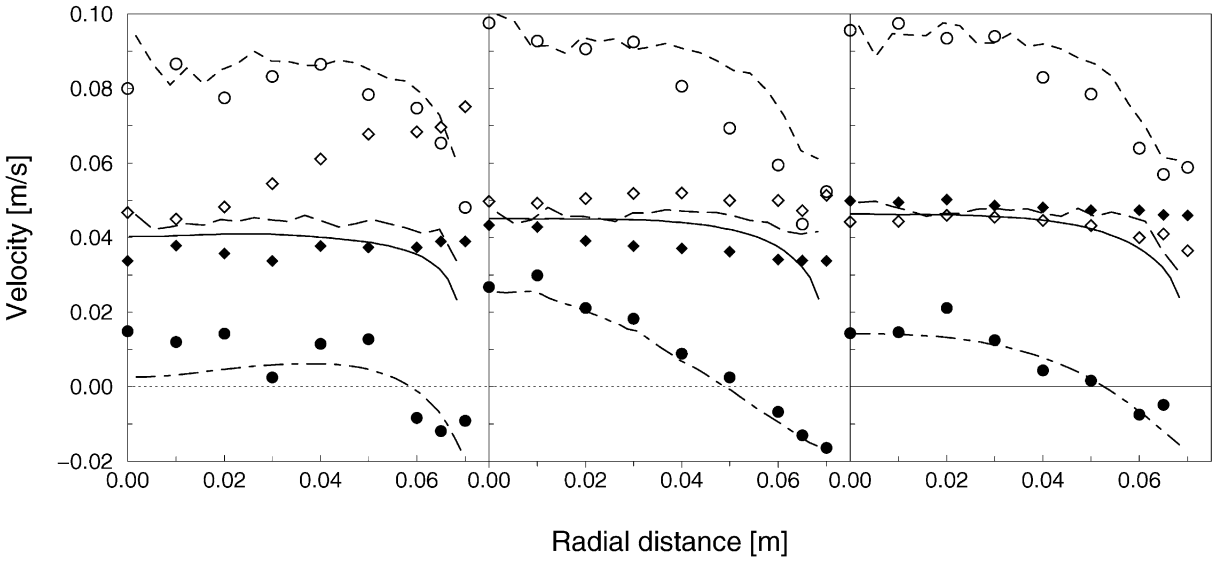

Fig. 10. Evolution along the buble column of the same variables as in Fig. 8 for the case of 0.37% gas volume fraction. $x = 100$ mm (left), $x = 300$ mm (centre) and $x = 480$ mm (right) above the aerator.

is found in all variables and in the three sections $x = 100$, 300, 480 mm considered, specially in the two upper ones.

6.2. Effect of the $C_{\varepsilon 3}$ coupling constant on the liquid flow

An illustration of the dependency of the topology of the liquid flow on the value of the coupling constant in the ε-equation, $C_{\varepsilon 3}$, is presented in Fig. 11. The same format as in Fig. 3 has been used.

Even for the relatively narrow interval of $C_{\varepsilon 3}$ values, namely $1.1 \leqslant C_{\varepsilon 3} \leqslant 1.8$, that has been considered, the changes in the flow field can be readily identified. For $C_{\varepsilon 3} = 1.1$ and 1.5, two large counter-rotating vortices in the upper and lower part of the column can be clearly distinguished. On the other hand, for $C_{\varepsilon 3} = 1.8$ there exists basically only one vortex extending to all of the bubble column, in agreement with the experiments. The presence of two large recirculating cells

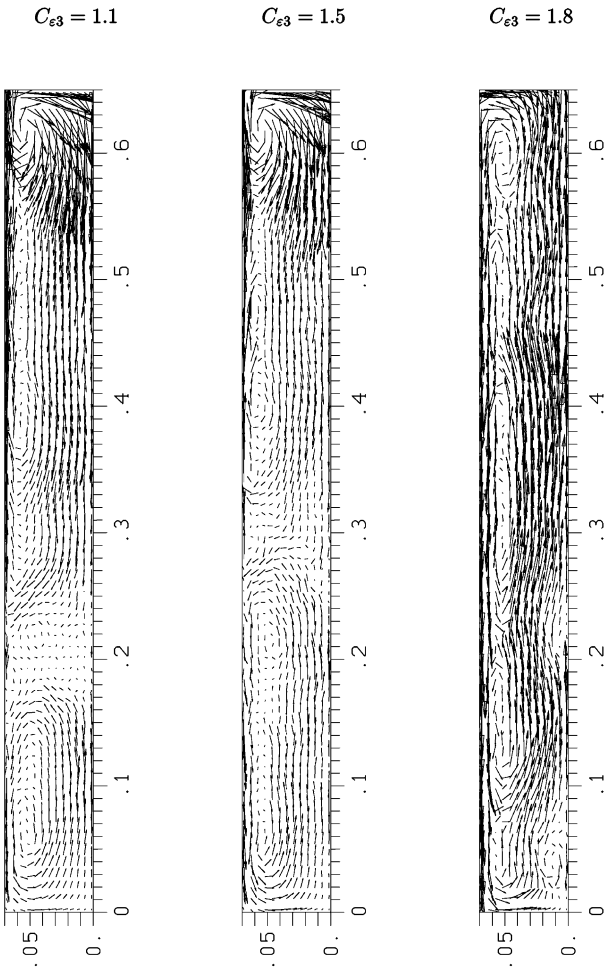

Fig. 11. Dependency of the liquid velocity field on the constant $C_{\epsilon 3}$ for the case 2 (87 l/h). Snapshots at the same computational time (600 s).

corresponds to an underprediction of the dissipation rate (represented by the smaller values of the $C_{\varepsilon 3}$, because the bubbles act as a source of dissipation). Therefore, the bubble radial fluctuating velocity values remain sufficiently large to favour a migration of the bubbles towards the wall. This induces a net upward liquid velocity near the wall and, as a consequence, a downward flow near the symmetry axis. As the value of $C_{\varepsilon 3}$ increases, the lower recirculating cell grows and eventually the upper one disappears. In conclusion, the qualitative changes happening in a narrow interval of $C_{\varepsilon 3}$ values indicate that the equilibrium between production and dissipation of pseudo-turbulence is quite delicate and is strongly affected by the modelling of the influence of the bubbles in the ε-equation.

6.3. Analysis of the contributions in the liquid-phase equations

As a method to get more insights into the underlying mechanisms governing the exchange of momentum and fluctuating kinetic energy between the bubbles and the liquid, the Eulerian transport equations for the liquid phase are divided into their five global contributions:

$$\text{Temporal} + \text{Convection} = \text{Diffusion} + \text{Source} + \text{Interaction}$$

The *temporal* denomination corresponds to the explicit time derivative of a variable ϕ, *convection* stands for the terms that describe the convective transport of ϕ, and *diffusion* for the corresponding diffusive transport. The source terms have been split into two categories according to their origins, namely the *source* and *interaction* terms which are identified with the symbols S_ϕ and $S_{\phi \mathrm{B}}$ of Table 1.

The radial variation of these contributions to the axial and radial liquid momentum equations as well as to the equations describing the liquid turbulent kinetic energy and its dissipation rate is shown in Figs. 12–19. Again, the evaluation was performed at the upper cross-section corre-

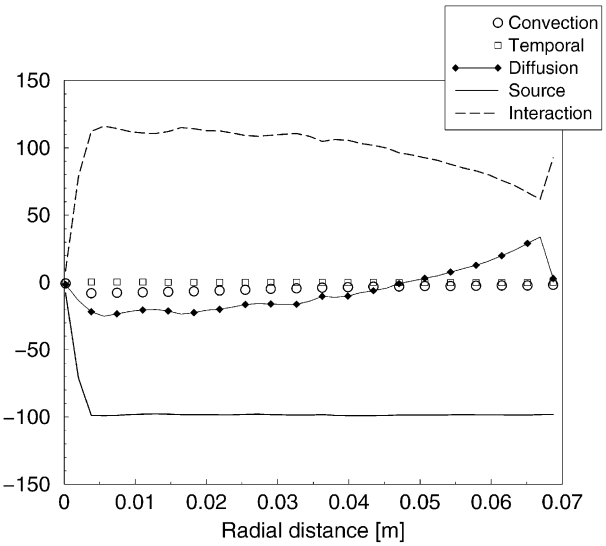

Fig. 12. The time-averaged constitutive terms [$m^2\ s^{-2}$] contributing to the axial momentum equation of the liquid. Case 87 l/h, 200 s time averaging.

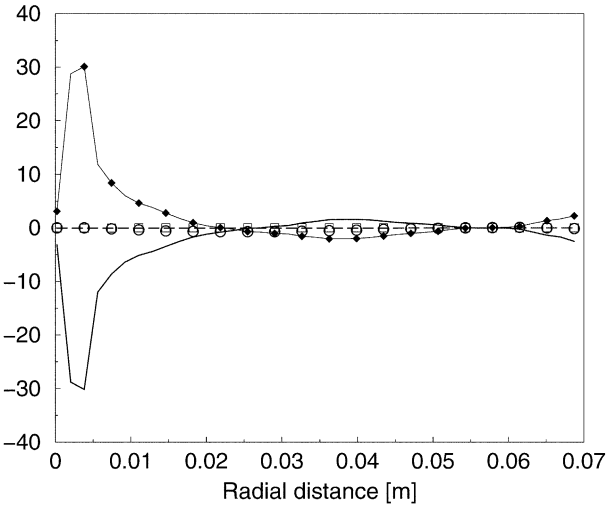

Fig. 13. The time-averaged constitutive terms [$m^2 s^{-2}$] contributing to the radial liquid momentum equation. Legend see Fig. 12.

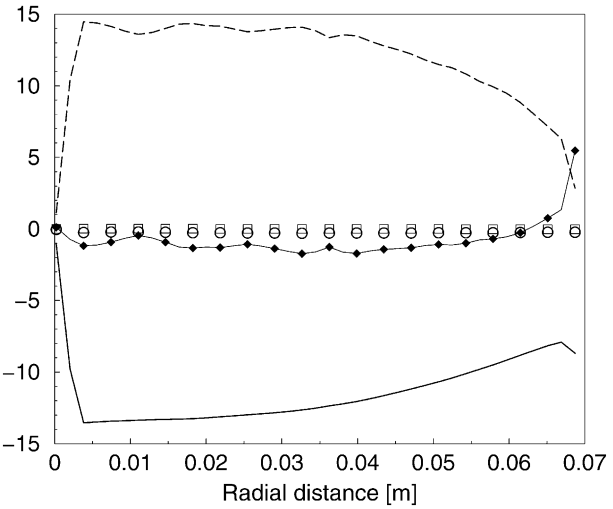

Fig. 14. The time-averaged constitutive terms [$m^2 s^{-3}$] contributing to the equation for the fluctuating kinetic energy of the liquid. Legend see Fig. 12.

sponding to 480 mm above the aerator. Instantaneous and time-averaged quantities are presented for each liquid variable in the case of 1.31% void fraction.

Figs. 12–15 present the relative weight of each contribution in the differential equations for U, V, k, and ε, respectively, averaged over 200 s. A general feature of all these graphs is that the *temporal* terms are quite close to zero and do not play any important role, showing that a statistical pseudo-stationary regime has been achieved. Also the averaged *convection* terms are small

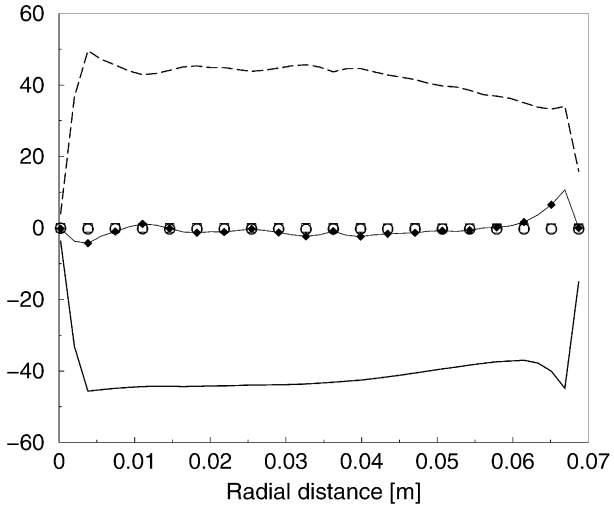

Fig. 15. The time-averaged constitutive terms [$m^2 s^{-4}$] contributing to the equation for the dissipation rate of fluctuating kinetic energy of the liquid. Legend see Fig. 12.

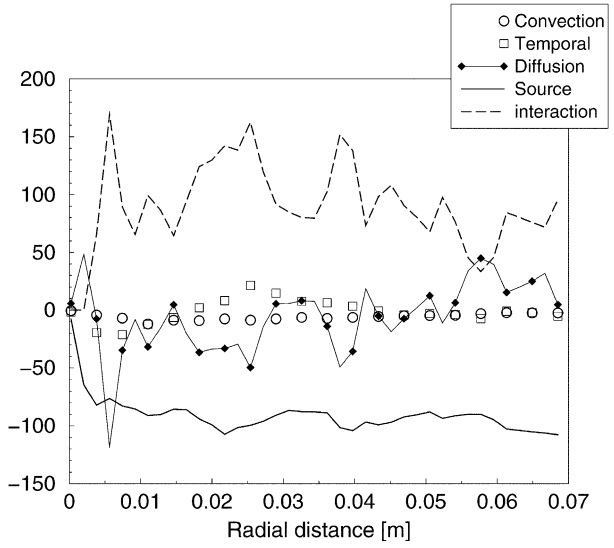

Fig. 16. Snapshot of the instantaneous constitutive terms [$m^2 s^{-2}$] in the equation for the axial velocity of the liquid. Case 87 l/h, after 600 s of simulation.

regarding other contributions as *source* or *interaction*. Once more it is necessary to point out that the calculations are unsteady with a time resolution governed by Δt_E.

In Fig. 12, corresponding to the axial liquid momentum equation, the bubbles act as a source of momentum which is compensated by the pressure and the body forces, accompanied by small modulations due to the *diffusion* term. This result was expected, because the motion of the liquid is

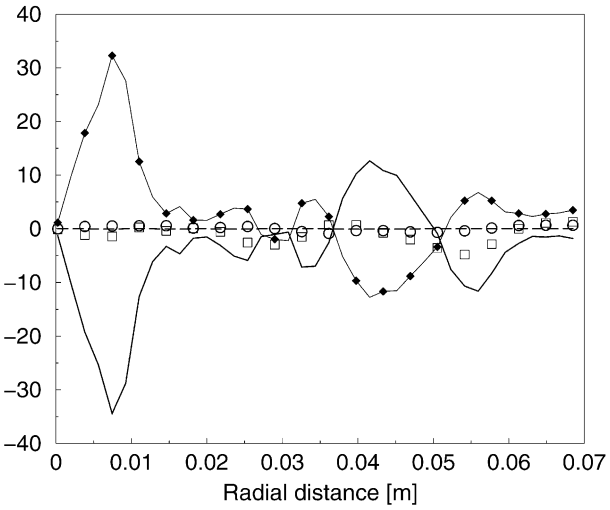

Fig. 17. Snapshot of the time-averaged constitutive terms [$m^2 s^{-2}$] in the equation for the radial velocity of the liquid. Legend see Fig. 16.

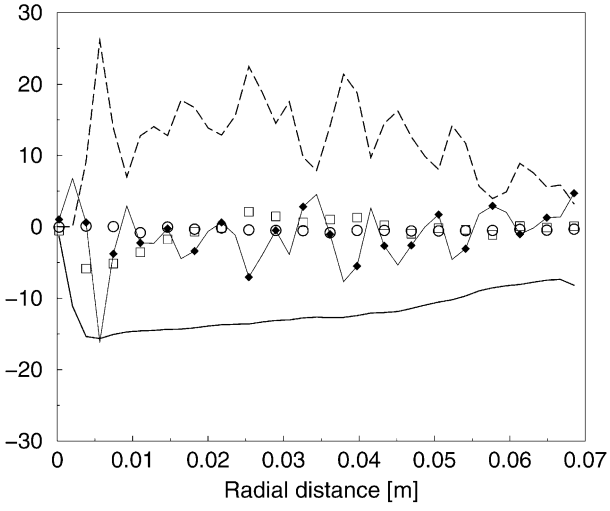

Fig. 18. Snapshot of the instantaneous constitutive terms [$m^2 s^{-3}$] in the equation for the fluctuating kinetic energy of the liquid. Legend see Fig. 16.

exclusively due to the momentum transfer from the bubbles. The case of the radial liquid velocity is somewhat different (Fig. 13), because the main equilibrium is established between the *source* and *diffusion* influences. The interaction term plays a minor role here. It is necessary to point out that the peak of the *source* and *diffusion* contributions near the symmetry axis is due to the inclusion of the term $-2(\mu + \mu_t)V/r^2$, that appears in axisymmetric equations, in the *source* term. As could be expected, the shape of the different contributions in the k- and ε-equations (Figs. 14 and 15) is quite similar to that in the U equation. The main balance is established between *interaction* and

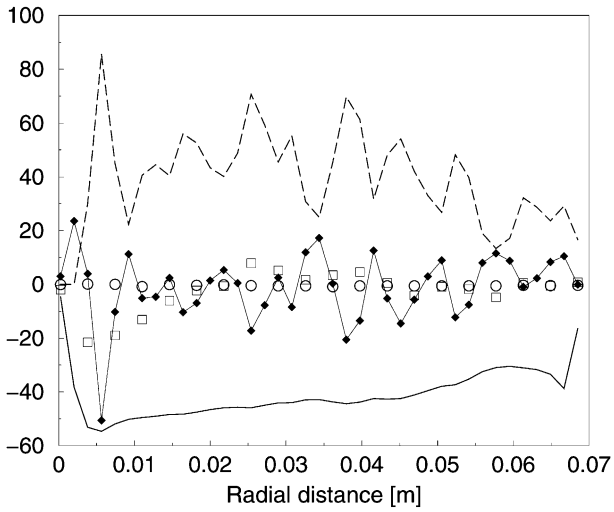

Fig. 19. Snapshot of the instataneous constitutive terms [$m^2\,s^{-4}$] in the equation for the dissipation rate of fluctuating kinetic energy of the liquid. Legend see Fig. 16.

source with a modulation due to *diffusion*. After examination of all these diagrams, the following conclusions can be extracted:

1. The bubbles act as a source of axial momentum, fluctuating kinetic energy and dissipation rate ε for the liquid. This is consistent with the intuitive idea that the changes in the liquid field are due to the action of the bubbles.
   On the other hand, the main contribution to $S_{k\mathrm{B}}$ is the drag force. In the *standard terms* this force leads to a term proportional to $-\left(\overline{u_i'u_i'} - \overline{u_i'u_{\mathrm{B}i}'}\right)$ which is negative, thus predicting a reduction of the liquid turbulence (Gouesbet and Berlemont, 1999) which is, obviously, not correct in the bubble column configuration. It should be remembered that the *standard terms* always subtract energy from the carrier flow, a feature which is obviously not true in the present situation.
2. The spatial variations of the liquid velocities (entering mainly in *convection* and *diffusion*) are small compared to the *interaction* and *source* terms in the time-averaged sense. This means that the production contribution in the k- and ε-equations is much smaller than the dissipation. From Fig. 14 it can be concluded that due to the effect of the bubbles $\varrho\varepsilon \approx S_{k\mathrm{B}}$, and from Fig. 15 it is possible to estimate:

$$C_2\varrho\varepsilon\frac{\varepsilon}{k} \approx C_{\varepsilon 3}\frac{\varepsilon}{k}S_{k\mathrm{B}} \Rightarrow C_2 \approx C_{\varepsilon 3}$$

   Therefore, the values for C_2 and $C_{\varepsilon 3}$ must be similar. In fact, $C_2 = 1.92$ and $C_{\varepsilon 3} = 1.8$ in this work, which constitutes an a posteriori consistency test. The main role of the $C_{\varepsilon 3}$ coefficient for the pattern of the liquid flow becomes clear now, because it controls directly the rate of dissipation of liquid turbulent kinetic energy generated by the bubbles.

The instantaneous behaviour of the global contributions can be quite different from the trends shown by the time-averaged values. This is illustrated in Figs. 16–19 for a certain time (after 600 s of simulation). The *interaction* term has an oscillatory shape instead of a smooth one due to the unsteady nature of the phenomenon. The counterbalance to this behaviour is provided by the *diffusion* contribution, which implies that the instantaneous spatial variations of the liquid velocity are relatively large. This behaviour is a reflection of the temporal change of the liquid velocity field, which evolves in time with a resolution governed by Δt_E. Such variations remain small in the time-averaged sense only, but perform oscillations of appreciable amplitude in instantaneous configurations of the liquid field. In addition, it can be noticed that the instantaneous *convection* and *temporal* contributions are small but not negligible against the others. The same comments as before are valid for the contributions in the radial liquid momentum equation.

7. Conclusions

In this paper, a Lagrangian-consistent formulation of the source terms due to the bubbles in the k- and ε-equations has been presented. In these source terms all the contact forces (drag, pressure gradient, added mass, transverse lift) considered in the bubble equation of motion have been included in a natural way to influence the turbulent quantities. Special attention has been given to the exchange of momentum and fluctuating energy between both phases. This objective has been achieved dividing the transport equations for the liquid variables into their specific contributions (temporal, convection, diffusion, source and interaction) and analysing the balances that appear in an instantaneous and the time-averaged situation. As a main result, the bubble source is directly responsible (in a time-averaged sense) for the production and dissipation of liquid fluctuating kinetic energy. This fact means that the modelling of the bubble source terms in the k- and ε-equations is the main issue to be solved in order to correctly predict the hydrodynamic behaviour of a bubble column, an issue that is currently under research. An illustration of the dependency of the liquid flow topology on the modelling of the action of the bubbles in the ε-equation has also been presented. Finally, the results of numerical simulations have been compared quantitatively with experimental data and have been found to provide reasonable and promising agreement in the mean and fluctuating velocities of both the liquid and bubble phase.

Acknowledgements

The financial support of the the present studies by the Deutsche Forschungsgemeinschaft under contract So 204/13 is gratefully acknowledged. The first author acknowledges the support by the Commission of the European Communities in the frame of a Marie Curie Research Training Fellowship (contract no. CT-97-2206).

References

Aliod, R., Dopazo, C., 1990. A statistically conditioned averaging formalism for deriving two-phase flow equations. Part. Part. Syst. Charact. 7, 191–202.

Becker, S., Sokolichin, A., Eigenberger, G., 1994. Gas–liquid flow in bubble columns and loop reactors: Part II. Comparison of detailed experiments and flow simulations. Chem. Eng. Sci. 49, 5747–5762.

Bröder, D., Sommerfeld, M., 1998. Simultaneous measurements of continuous and dispersed phase in bubble columns by PDA. In: Proceedings of 9th International Symposium on Applications of Laser Techniques to Fluid Mechanics, Lisbon, Portugal, July.

Bröder, D., Laín, S., Sommerfeld, M., 2000. Experimental studies fo the hydrodynamics in a bubble column. In: Proceedings of 5th German–Japanese Symposium on Bubble Columns TU Bergakademie Freiberg, pp. 125–130.

Bunner, B., Tryggvason, G., 1998. Direct numerical simulation of large three-dimensional bubble systems. In: Proceedings of the 1998 ASME Fluids Engineering Division Summer Meeting, Washington, June.

Bunner, B., Tryggvason, G., 1999. Direct numerical simulations of three-dimensional bubbly flows. Phys. Fluids. 11, 1967–1969.

Bunner, B., 2000. Numerical simulation of gas–liquid bubbly flows. Ph.D. Thesis, University of Michigan, Ann Arbor, USA.

Crowe, C.T., 2000. On models for turbulence modulation in fluid-particle flows. Int. J. Multiphase Flow 26, 719–727.

Crowe, C.T., Gillandt I., 1998. Turbulence modulation of fluid-particle flows. A basic approach. In: Proceedings of the 3rd International Conference on Multiphase Flow, Lyon, France, June.

Crowe, C.T., Sharma, M.P., Stock, D.E., 1977. The particle-source-in-cell (PSI-cell) method for gas-droplet flows. J. Fluids Eng. 99, 325–332.

Delnoij, F.A., Kuipers, J.A.M., van Swaaij, W.P.M., 1997a. Computational fluid dynamics applied to gas–liquid contactors. Chem. Eng. Sci. 52, 3623–3638.

Delnoij, E., Lammers, F.A., Kuipers, J.A.M., van Swaaij, W.P.M., 1997b. Dynamic simulation of dispersed gas–liquid two-phase flows using a discrete bubble model. Chem. Eng. Sci. 52, 1429–1458.

Delnoij, F.A., Kuipers, J.A.M., van Swaaij, W.P.M., 1997c. Dynamic simulation of gas–liquid two-phase flow: Effect of column aspect ratio on the flow structure. Chem. Eng. Sci. 52, 3759–3772.

Devanathan, N., Dudukovic, M.P., Lapin, A., Lübbert, A., 1995. Chaotic flow in bubble column reactors. Chem. Eng. Sci. 50, 2661–2667.

Esmaeeli, A., Tryggvason, G., 1999. Direct numerical simulations of bubbly flows. Part II: Moderate Reynolds number arrays. J. Fluid Mech. 385, 325–358.

Février, P., Simonin, O., 1998. Constitutive equations for fluid-particle velocity correlations in gas–solid turbulent flows. In: Proceedings of the 3rd International Conference on Multiphase Flow, Lyon, France, June.

Gouesbet, G., Berlemont, A., 1999. Eulerian and Lagrangian approaches for predicting the behaviour of discrete particles in turbulent flows. Prog. Energy Combust. Sci. 25, 133–159.

Göz, M.F., Sundaresan, S., 1998. The growth saturation, and scaling behaviour of one- and two-dimensional disturbances in fluidized beds. J. Fluid Mech. 362, 83–119.

Göz, M.F., Bunner, B., Sommerfeld, M., Tryggvason, G., 2000. Direct numerical simulation of the interaction of gas bubbles in a liquid—the effects of deformability and bidispersity. In: Proceedings of the 5th German–Japanese Symposium on Bubble Columns, Dresden, May.

Hyland, K., Simonin, O., Reeks, M.W., 1998. On the continuum equations for two-phase flows. In: Proceedings of the 3rd International Conference on Multiphase Flow, Lyon, France, June.

Ishii, M., 1975. Thermo-Fluid Dynamic Theory of Two-Phase Flow. Eyrolles, Paris.

Ishii, M., 1990. Multiphase science and technology, vol. 5, Chapter 1. In: Hewitt, G.F., Delhaye, J.M., Zuber, N. HPC, Washington, DC.

Jackson, R., 1997. Locally averaged equations of motions for a mixture of identical spherical particles and a Newtonian fluid. Chem. Eng. Sci. 52, 2457–2469.

Kenning, V.M., Crowe, C.T., 1997. On the effect of particles on carrier phase turbulence in gas-particle flows. Int. J. Multiphase Flow 23, 403–408.

Kohnen, G., 1997. On the influence of phase interactions in turbulent two-phase flows and their numerical implementation within the Euler–Lagrange approach (in german). Ph.D. Thesis, University Halle-Wittenberg, Germany.

Laín, S., Bröder, D., Sommerfeld, M., 1999. Experimental and numerical studies of the hydrodynamics in a bubble column. Chem. Eng. Sci. 54, 4913–4920.

Laín, S., Göz, M.F., 2001. Numerical instabilities in bubble tracking in two-phase flow simulations. Int. J. Bifurcation and Chaos 11, 1169–1181.

Lapin, A., Lübbert, A., 1994. Numerical simulation of the dynamics of two-phase gas–liquid flows in bubble columns. Chem. Eng. Sci. 49, 3361–3674.

Launder, B.E., Spalding, D.B., 1974. The numerical computation of turbulent flows. Comp. Meth. Appl. Mech. Eng. 3, 269–289.

Lin, T.J., Reese, J., Hong, T., Fan, L.S., 1996. Quantitative analysis and computation of two-dimensional bubble columns. AIChE J. 42, 301–318.

Mudde, R.F., Lee, D.J., Reese, J., Fan, L.S., 1997. Role of coherent structures on Reynolds stresses in a 2-D bubble column. AIChE J. 43, 913–926.

Pan, Y., Dudukovic, M.P., Chang, M., 1999. Dynamic simulation of bubble flow in bubble columns. Chem. Eng. Sci. 54, 2481–2489.

Prosperetti, A., Zhang, D.Z., 1994. Averaged equations for insviscid disperse two-phase flow. J. Fluid Mech. 267, 185–219.

Reeks, M.W., 1993. On the constitutive relations for dispersed particles in non-uniform flows. I. Dispersion in a simple shear flow. Phys. Fluids A 5, 750–761.

Sanyal, J., Vásquez, S., Roy, S., Dudukovic, M.P., 1999. Numerical simulation of gas–liquid dynamics in cylindrical bubble column reactors. Chem. Eng. Sci. 54, 5071–5083.

Shirolkar, J.S., Coimbra, C.F.M., Queiroz McQuay, M., 1996. Fundamental aspects of modeling turbulent particle dispersion in dilute flow. Prog. Energy Combust. Sci. 22, 363–399.

Simonin, O., 1990. Eulerian formulation for particle dispersion in turbulent two-phase flows. In: Proceedings of the 5th Workshop on Two-Phase Flow Predictions, Erlangen, Germany, March.

Sokolichin, A., Eigenberger, G., 1994. Gas–liquid flow in bubble columns and loop reactors: Part I. Detailed modelling and numerical simulation. Chem. Eng. Sci. 49, 5735–5746.

Sokolichin, A., Eigenberger, G., 1999. Applicability of the standard k–ε turbulence model to the dynamic simulation of bubble columns: Part I. Detailed numerical simulations. Chem. Eng. Sci. 54, 2273–2284.

Sommerfeld, M., Kohnen, G., Rüger, M., 1993. Some open questions and inconsistencies of Lagrangian particle dispersion models. Proceedings of the Ninth Symposium on Turbulent Shear Flows, Kyoto, August. Paper 1S.1.

Sommerfeld, M., 1996. Modellierung und numerische Berechnung von partikelbeladenen turbulenten Strömungen mit Hilfe des Euler/Lagrange Verfahrens (Modelling and numerical calculation of turbulent flows laden with particles by means of the Euler/Lagrange procedure), Habilitation Thesis, University Erlangen-Nürnberg, Shaker Verlag, Aachen.

Squires, K.D., Eaton, J.K., 1992. On the modelling of particle-laden turbulent flows. In: Proceedings of the 6th Workshop on Two-Phase Flow Predictions, Erlangen, Germany, April.

Tzeng, Y.B., Chen, R.C., Fan, L.S., 1993. Visualization of flow characteristics in a 2D bubble column and three-phase fluidized bed. AIChE J. 39, 733–744.

Yuan, Z., Michaelides, E.E., 1992. Turbulence modulation in particulate flows—a theoretical approach. Int. J. Multiphase Flow 18, 779–785.

Zaichik, L.I., Alipchenkov, V.M., 1999. A kinetic model for the transport of arbitrarydensity particles in turbulent shear flows. In: Proceedings of Turbulence and Shear Flow Phenomena 1, Sta. Barbara CA, USA.